ADVANCES IN ATMOSPHERIC SCIENCES, VOL. 21, NO. 5, 2004, 775–783

Physicochemistry and Mineralogy of Storm Dust and Dust Sediment in Northern China

LIU Wei (刘 蔚), FENG Qi* (冯 起), WANG Tao (王 涛),
ZHANG Yanwu (张艳武), and SHI Jianhua (施建华)

Cold and Arid Regions Environmental and Engineering Research Institute,
Chinese Academy of Sciences, No. 260 West Dong Gang Road, Lanzhou 730000

(Received 23 June 2003; revised 8 May 2004)

ABSTRACT

Dust sediments collected from 1995 to 1998 in Beijing, Dunhuang, Inner Mongolia, Kashi, the Kunlun Mountains, Lanzhou, Ningxia, the Taklimakan Desert, and Xi'an, China, were characterized in terms of their physical, chemical, and mineralogical properties. Most aerosols and dust analysed ranged in texture from silty clay to clay loam. Their median particle diameters (Mds) generally ranged between 5 to 63 μm, coinciding with those of loess from central China and the finest sand from northwestern China. The dust sediments were characterized by a predominance of SiO_2 and Al_2O_3, followed by K_2O. Their SiO_2/Al_2O_3 and K_2O/SiO_2 molar ratios ranged from 5.17 to 8.43 and from 0.009 to 0.0368, respectively. The mass concentration spectrum during a dust storm showed a single peak, rather than the triple peak generally observed under clear sky conditions. The dominant minerals were chlorite, illite, calcite, and dolomite. These physical, chemical, and mineralogical properties were consistent with those of aeolian soils and loess in western and central China. The results suggest that aerosols and fine-grained fractions of dust sediments collected in northern China are mainly composed of soil material transported from the arid and semiarid regions of China and Mongolia by prevailing winds. The rate of deposition and properties of dust falling on eastern China were strongly influenced by meteorological conditions, season, latitude, longitude, and altitude of the sampling sites.

Key words: physical chemistry and mineralogy, dust storm, dust sediment, northern China

1. Introduction

Dust storms, defined by wind velocities exceeding 17 m s^{-1} and visibility under 1000 m, occur with great frequency and magnitude in the world's arid and semi-arid regions (Goudie, 1978; Yaalon and Dan, 1974; Yaalon and Ganor, 1973). Desert dust, an estimated 500 Tg yr^{-1} worldwide (Naruse et al., 1986), is frequently transported over hundreds of kilometers. The most severe dust storms, which can carry fine particles over thousands of kilometers, originate in such great desert regions as the Sahara and Northwest China (Pewe, 1981). The world's major deserts and the surrounding arid and semi-arid lands, where this dust originates, cover 4.33×10^7 km^2 or 36% of the Earth's landmass (Meigs, 1953). In Asia, spring frontal activities in Northeast and North China are the origin of the fairly widespread transport of particles over northern China (Fan et al., 1996). In recent dust storm studies, measurements of dust grain size have indicated that this dust originates mainly in the arid and semi-arid areas of the Loess Plateau of northern and northwestern China. Dust also originates in the northeastern portion of the Gansu Corridor, in western Inner Mongolia, including the arid deserts and Gobi, and in the Taklimakan Desert of South Xinjiang. Circulation from the East Asian winter monsoon is an important agent for dust transport (An et al., 1990; Zhang et al., 1994, 1999). Li et al. (1998) established that narrow region or valley between mountain ranges of the Hexi Corridor contribute greatly to strong airflows and dust transport. The greatest frequency of dust storms occurs between March and April, influenced by depressions or troughs over dust storm-originating regions where upward flow prevails.

Most studies have not dealt with the phase composition of dust samples, studying only their elemental

*E-mail: qifeng@ns.lzb.ac.cn

composition, and that generally for only a single compound or mineral (David and Guo, 2000). Thus, the composition of dust and its pattern of transport remain unclear. During the period of March 1995 to May 1998, several mineral dust deposition events occurring in eastern China were recorded, namely in Beijing, Dunhuang, Inner Mongolia, Kashi, Lanzhou, Ningxia, the Taklimakan Desert, the Kunlun Mountains, and Xi'an. The rather low deposition mass ($< 0.10\,\mathrm{g\,m^{-2}}$), recorded locally during individual washout events, did not preclude dust storms from having an influence as far away as Japan and the American West, where some fallout events were recorded (Zhang et al., 1999). Two of the dust storms investigated were severe, with gust velocities exceeding $20\,\mathrm{m\,s^1}$ and visibility falling below 200 m.

The current study seeks to analyze the deposition characteristics of dust in recent times. In addition, the study of the physical, chemical, and mineralogical characteristics of aerosols and deposited sediments from a number of locations will provide background information for further research.

2. Methodology

A total of 90 ground-based, size-separated dust particle samples were collected at nine sites (Beijing, Dunhuang, Inner Mongolia, Kashi, Lanzhou, Ningxia, the Taklimakan Desert, the Kunlun Mountains, and Xi'an) between March and June 1994 and between March and May 1998. Of the ten sets of nine spatially distributed samples, nine were collected during dust storm periods, and one under clear sky conditions. Sampling intervals ranged from 10 to 72 h.

Single orifice, 8-stage, Battelle-type cascade inspectors provided 8 particle-size fractions (< 0.25, 0.25–0.5, 0.5–1.0, 1.0–2.0, 2.0–4.0, 4.0–8.0, 8.0–16.0 and >16.0 μm aerodynamic equivalent diameter) and were used for sampling during the dust deposition events. Equipped with a 3.5 μm thick Mylar impaction surface, the samplers were further equipped with a 0.4 μm porosity Millipore backup filter, resulting in a flow rate of roughly 11 particles per minute. The determination of the range and distribution of dust grain size was carried out by analysing randomly selected scanning electron microscope (SEM) micrographs produced from individual samples (Smart and Tovery, 1981). All particles on a given micrograph were measured (400–1400 counts per sample) and grain size classes expressed on a percentage basis.

The mineralogical composition of the material was determined by X-ray diffractometry of both tube (aerosol) and sedimentation samples. Samples (200 mg) were oven-dried at 110 EC and then heated to 950 EC for twelve hours. The ignition loss (IL) was calculated as the weight lost between 110 and 950 EC. After fusing the samples with Na_2CO_3, the SiO_2 contents were determined gravimetrically. The Al_2O_3 and Fe_2O_3 contents were determined by the ferron method (Davenport, 1949). The CaO, MgO, and MnO contents were determined by atomic absorption, the latter after sample digestion with HF-H_2SO_4. The TiO_2 and P_2O_5 contents were determined colorimetrically, while the K_2O and Na_2O contents were determined by flame photometry (Inoue and Naruse, 1987). An X-ray fluorescence analyzer (XRF; RIGAKU model RIX2000: RH cathode: 50 kV–50 mA) was used to measure sediment Cu, Zn, and Pb (Yamazaki et al., 2001). Element Ni, Co, and Cr contents were determined using the Mehlich-III method (Mehlich, 1984). A 2.5-g air-dried fraction sample was weighed out into a 50 mL polystyrene centrifuge tube, 25 mL of Mehlich-III extractant was added, and the suspension was shaken for 5 min, then filtered through Whatman 42 filter paper. Concentrations of metals in the filtrate were analyzed using an Inductively Coupled Plasma Atomic Emission Spectrometer (ICP-AES, Ultima, JY Horiba Inc., Edison, NJ). Further analyses included direct-beam X-ray transmission (XRT) analysis for the detemination of mass attenuation coefficients, and X-ray diffraction scanning with Cu and K using a graphite monochromator. Mineral identification and particle sizing was performed with a polarizing optical microscope (Davis and Guo, 2000) equipped with a spectral actinometer which allowed the full range of solar radiation to be used.

3. Variations in dust storm frequency and intensity

The earliest recorded dust event in China occurred in 1150 BCE (Before Century) (Wang, 1963), but much more detailed information is available for events of the last 1000 years (An and Liu, 1984). Places where dust falls occurred in historic times are shown in Fig. 1. The greatest frequency of dust fall events occurred during 1060–1090, 1160–1270, 1470–1560, 1610–1700, and 1820–1890, and from 1997 to 2000 (Feng et al., 2004). The variation in dust storm frequency by year as described by various regression equations (linear, logarithmic, polynomial, and exponential) suggests that, based on 1100 dust storms examined, their frequency of occurrence has increased over time ($R^2 > 0.16$; Table 1; Feng et al., 2004). The greatest frequency of dust falls occurs in March through May, with April account-

Table 1. Regression functions relating annual dust storm frequency (y) and year (x) for the years 300 to 2000 A.D.

Regression type	Regression functions	Indexes
Linear	$y = 0.0018x + 0.1174$	R^2=0.2046
Logarithmic	$y = 1.6681 \ln x - 9.327$	R^2=0.1611
Polynomial	$y = 2\times10^{-6}x^2 - 0.0031x + 2.5751$	R^2=0.2531
Exponential	$y = 0.8323\mathrm{e}^{0.0007x}$	R^2=0.2275

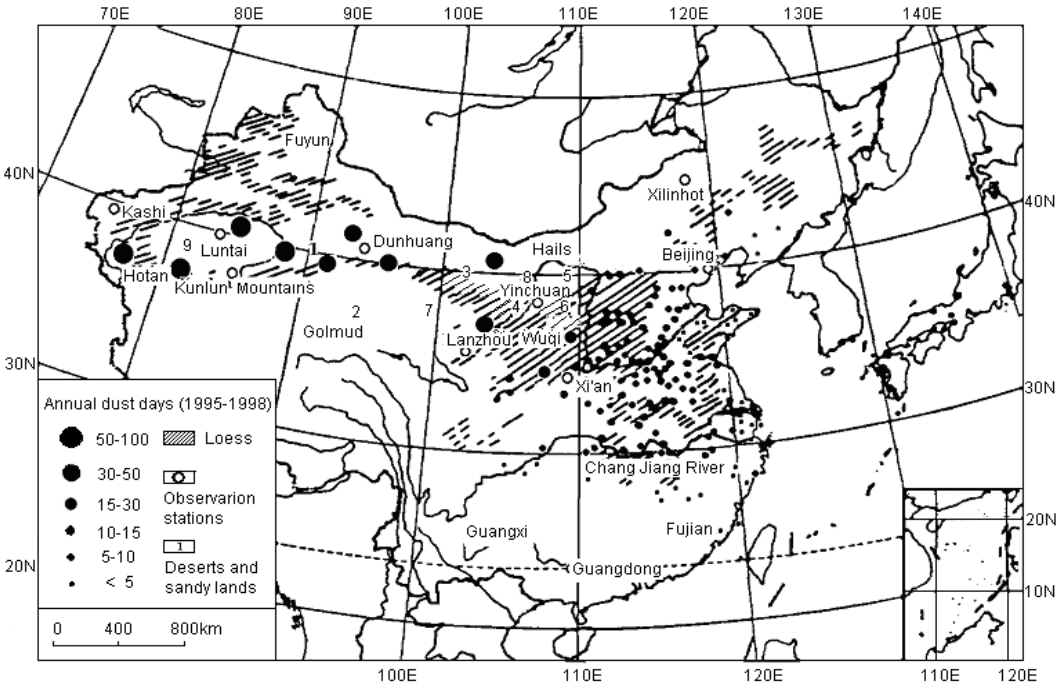

Fig. 1. Distribution and frequency of dust storms in China along with fallen dust and loess sampling locations in China. 1. Kumtag Desert; 2. Deserts in Qaidam Basin; 3. Badain Jaran Desert; 4. Tengger Desert; 5. Hobq Desert; 6. Mu Us Sandy Lands; 7. Hexi Corridor; 8. Helan Mountains; 9. Taklimakan Desert (figure modified from Zhang, 1980).

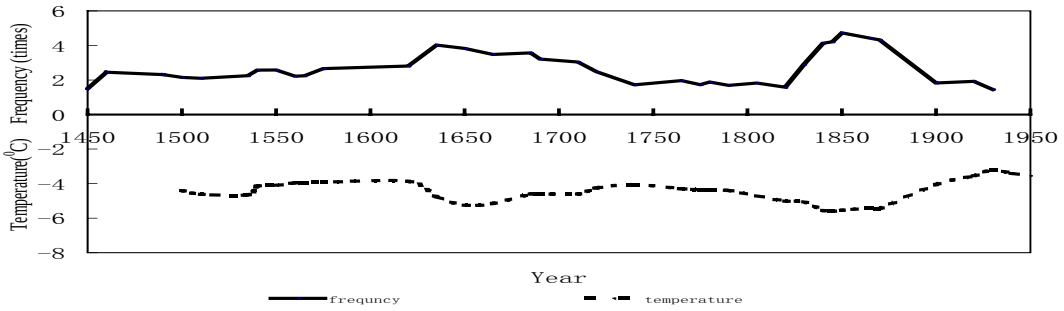

Fig. 2. Relationships between annual dust storm frequency and the temperature index (dotted line) for Beijing, 1500–2000 A. D.

ing for 26% of the annual total. Over the period studied, the yearly mean temperature index was inversely related to dust storm frequency (Fig. 2; Zhang, 1980), with the greatest frequency of dust storm events occurring during cold periods in northern China. A plot of dust storm event frequency versus humidity index over the last 2000 year for the region of China situated between 35°–40°N (Zhen, 1973) indicates that most of the periods of high dust-fall event frequency correspond with dry spells. This supports Liu's explanation that aeolian losses from loess leads to silt deposition under dry climatic conditions (Liu, 1964, 1982).

It is interesting to note that a number of main dust storm events of the recent past have coincided with the occurrence of El Niño events: (1) dust storm: 9 September 1952; El Niño: August 1951 to April 1952, (2) dust storm: 22 April 1977; El Niño: June 1976 to March 1977, (3) dust storm: 28 April 1983; El Niño: September 1982 to September 1983, (4) dust storm: 5 May 1993; El Niño: April 1993 to December 1993. Given this evidence, the large-scale environmental conditions occurring under El Niño conditions are considered an important factor contributing to strong dust storm activity (Chen, 1993). However, further evidence needs to be gathered to elucidate this rela-

Table 2. Size distribution of dust particles collected in northern China in 1994.

Sampling site	Grain-size (μm)	Md*(μm)	S_o	S_k	Kur
Kashi	200–0.2	23.21	1.27	0.756	3.802
Kunlun Mountains	80–1.0	23.13	1.17	1.319	5.557
Taklimakan Desert (Luntai)	200–2	93.54	1.43	0.117	2.316
Dunhuang	50–2	17.49	0.52	2.398	7.963
Lanzhou	100–0.3	17.12	1.55	0.397	3.960
Xi'an	80–0.2	20.00	0.85	0.966	4.480
Ningxia (Yinchuan)	80–0.4	20.73	1.81	0.291	1.898
Inner Mongolia (Xilinhot)	80–0.3	10.15	1.08	1.031	2.878
Beijing	50–0.2	3.97	0.34	1.176	8.693

*Md: the median diameter of sample (μm); S_o: the mean sorting coefficient of sample; S_k: standard deviation; Kur: kurtosis.

Table 3. Chemical compositions of dust samples collected at nine locations in northern China in 1994.

Locations	IL* (%)	SiO_2 (%)	Al_2O_3 (%)	Fe_2O_3 (%)	TiO_2 (%)	MnO (%)	CaO (%)	MgO (%)	Na_2O (%)	K_2O (%)	P_2O_5 (%)	SiO_2/Al_2O_3	K_2O/SiO_2
Kashi	—	56.2	8.27	3.64	0.53	0.07	10.46	2.88	2.76	2.07	0.17	6.79	0.0368
Kunlun Mountains	—	61.3	8.18	4.90	0.47	0.07	9.8	2.78	2.75	1.34	0.20	7.49	0.0219
Taklimakan Desert (Luntai)	—	77.21	10.17	2.20	0.38	0.05	2.65	2.87	12.52	1.73	0.22	7.59	0.0367
Dunhuang	3.77	75.77	9.21	2.60	0.12	0.04	2.56	1.17	2.07	1.55	0.07	8.22	0.0205
Lanzhou	—	59.3	11.47	4.04	0.60	—	5.96	1.32	2.17	1.20	0.20	5.17	0.0203
Xi'an	13.7	62.51	6.41	4.9	0.7	0.08	6.27	2.25	1.70	1.17	0.20	8.43	0.0187
Ningxia (Yinchuan)	4.91	66.79	9.07	5.48	0.46	0.09	1.64	1.62	2.26	1.21	0.11	7.36	0.0153
Inner Mongolia (Xilinhot)	—	71.23	11.15	4.83	0.70	—	5.36	1.14	2.1	0.77	0.10	6.39	0.0109
Beijing	2.68	63.5	10.41	5.63	0.58	0.15	0.73	1.54	2.53	0.57	0.07	6.10	0.009

*IL=ignition loss

tionship.

4. Sediment characteristics

4.1 *Physical characteristics of fallen dust*

Given that the particle diameters of tropospheric dust (6–10 km altitude) range from 1 to 100 μm, those of stratospheric dust are < 1 μm, and that the particles harvested at the nine sites in China were predominantly 1–50 μm in diameter (Table 2), it is concluded that the clayey to silt fractions of the dust sediments collected at ground level were mainly of tropospheric origin. The collected dust bore various amounts of sand (14%–65%). A poorly sorted particle size distribution was particularly evident in the Kashi and Lanzhou samples, indicating that they were composed of a wide range of particle sizes (Table 2). Most of the coarser fraction in these dust samples was associated with soil materials taken up from adjacent locations by the wind.

Table 2 shows that in China most dust sediments range in size from 5 to 63 μm. The mean diameter of grain size of dust captured in the Taklimakan and eastern sites ranged from 2 to 200 μm and 0.2 to 100 μm, respectively, the latter being poorly sorted compared to the former (Zhu and Cheng, 1994). The Md (median diameter) of dust captured in Xi'an near the Loess Plateau ranged from 0.2 to 80 μm, but was less than that of loess from the Loess Plateau (2–16 μm; Chen, 1993).

While the diameter of dust particles collected in Beijing on clear days was generally less than 4 μm, on dust storm days the dominant grain size of the aerosols ranged from 0.6 to 1.0 μm (Qian et al., 1997). An aerosol sample collected on the flat roof of a 10-m tall building in Beijing showed an Md of 3.9 μm and additionally, the mineral particles in the 0.3–0.5 μm size range show regular shapes, indicating their secondary reaction origin (Shi et al., 2003) (Table 2). The particle analysis presented in Table 2 is consistent with

Table 4. The EF value of dust sediments captured at nine locations in northern China.

Sampling site	Cu	Zn	Pb	Ni	Co	Cr	Mn	Fe	Ti	Ca	Mg	K	Na
Kashi	0.80	1.77	2.68	0.60	0.59	0.43	1.12	1.00	1.33	4.95	1.54	1.25	1.12
Kunlun Mountains	1.23	1.87	2.98	0.32	0.43	0.53	1.25	1.54	1.65	5.89	1.32	1.05	1.02
Taklimakan Desert (Luntai)	0.56	1.89	3.67	0.56	0.78	0.33	1.12	12.00	1.78	5.65	1.65	1.25	1.74
Dunhuang	0.73	1.93	17.00	0.67	0.6	0.70	1.10	11.00	1.36	4.89	1.91	1.21	0.87
Lanzhou	23.76	54.38	42.13	0.79	0.75	1.10	0.84	1.00	0.77	2.19	0.71	0.59	0.37
Xi'an	18.45	2.21	13.74	0.48	0.80	1.70	1.02	1.00	1.52	3.03	1.10	1.25	0.94
Ningxia (Yinchuan)	8.77	24.12	9.00	0.76	0.78	0.87	0.94	1.00	1.23	3.58	1.59	0.93	1.19
Inner Mongolia (Xilinhot)	24.00	63.42	35.11	1.00	0.80	0.80	1.00	1.00	1.39	2.32	1.00	1.23	0.90
Beijing	25.13	79.34	78.12	2.13	0.78	0.89	1.10	1.20	1.45	2.45	1.00	1.42	0.78
Base value of crust*	20	50	10	40	10	—	850	3.8	0.46	1.37	0.63	1.36	0.63

*From Liu (1985)

the observation that the longer the distance from the source, the lesser the Md of sediments and aerosols (Middleton et al., 1986; Prospero et al., 1987; Pye, 1987).

4.2 *Chemical characteristics of dust*

Dust trapped at the nine sampling sites showed a predominance of SiO_2 and Al_2O_3 (Table 3). The molar ratio of SiO_2/Al_2O_3 of dust samples ranged from 5.17 to 8.43, while that of Chinese loess ranged from 6.3 to 9.3. The quantity of K_2O in dust samples was low (0.57%–2.85%) and quite similar to that of Chinese loess (1.43%–3.09%). Likewise, the K_2O/SiO_2 molar ratios of the dust samples, ranging from 0.0090 to 0.0368, were also very similar to those of Chinese loess and aeolian soils (0.0130–0.0400) (Table 3). This suggests that the aerosols and dust collected in China were predominantly composed of fine soil particles transported from the Loess Plateau and its surroundings.

Based on the characteristics of eight of their chemical components, the origins of the dust samples collected in Xi'an and Beijing were identified. High CaO and Na_2O contents, low K_2O contents, and significant ignition losses characterized the Xi'an samples whereas the Beijing samples had a low CaO content and low ignition losses (Table 3).

Particulate matter in the air is composed of two fractions: (1) natural particles, including volcanic particles, salt particles from the sea, and aeolian particles, and (2) particles of industrial origin. The enrichment factor ($I_{\mathrm{EF},x}$) is often used as an index to analyze the sources of particulate matter:

$$I_{\mathrm{EF},x} = \frac{[\mathrm{X}]_{\mathrm{air}}}{[\mathrm{Fe}]_{\mathrm{air}}} \Big/ \frac{[\mathrm{X}]_{\mathrm{crust}}}{[\mathrm{Fe}]_{\mathrm{crust}}} ,$$

where $[\mathrm{X}]_{\mathrm{air}}$ is the concentration of a given element X in the airborne particles, $[\mathrm{Fe}]_{\mathrm{air}}$ is the concentration of Fe (iron) in the airborne particles, $[\mathrm{X}]_{\mathrm{crust}}$ is the concentration of a given element X in the Earth's crust, $[\mathrm{Fe}]_{\mathrm{crust}}$ is the concentration of Fe (iron) in the Earth's crust.

The relative concentration of X to Fe in the Earth's crust, $[\mathrm{X}]_{\mathrm{crust}}/[\mathrm{Fe}]_{\mathrm{crust}}$, has been previously determined (Liu, 1985). A value of $I_{\mathrm{EF},x} > 10$ for a given element indicates an artificial or industrial source, whereas a value of $I_{\mathrm{EF},x} < 10$ indicates a crustal source (Liu, 1985).

The I_{EF} values of dust samples collected at the nine sites are presented in Table 4. The main I_{EF} values of airborne particulate matter from aeolian fine sand and clay from on-site and nearby regions are shown. For most elements, the differences in $I_{\mathrm{EF},x}$ between spring and summer samples taken at the Kashi, Kunlun mountain, Tarim basin, and Dunhuang sampling sites were similar (Table 4). The $I_{\mathrm{EF},x}$ value for most elements and sites (particularly desert sites) was less than 10 and close to 1; that is to say that the concentration in airborne materials of most elements was similar to that in the crust. Elevated $I_{\mathrm{EF},x}$ values for Ca in westert parts are the result of a regionally elevated topsoil Ca content. The high $I_{\mathrm{EF},x}$ value for Pb in Dunhuang is due to the air pollution generated by a large tourist population. The fact that airborne particulates often come from nearby regions is further evidenced by the similar elemental distribution pattern of the clay in desert areas and airborne particulate in the air (Table 4).

The $I_{\mathrm{EF},x}$ value of some dust samples exceeded 10: (1) $I_{\mathrm{EF,\,Cu}}$ ranged from 8.45 in Xi'an to 25.13 in Beijing, (2) $I_{\mathrm{EF,\,Zn}}$ from 24.12 in Ningxia to 128.43 in Beijing, and (3) $I_{\mathrm{EF,\,Pb}}$ from 13.74 in Xi'an to 78.12 in Beijing. These elevated $I_{\mathrm{EF},x}$ values for materials

Table 5. Mineral type content of dust captured at nine sites in China (1994) based on X-ray powder diffractograms, expressed as a percentage of total mineral content.

Locations	Chlorite	Illite	Calcite	Dolomite	Gypsum	Zeolite
Kashi	8	13	13	10	—	3
Kunlun Mountains	8	9	11	9	2	3
Taklimakan Desert (Luntai)	10	8	15	7	3	5
Dunhuang	8	14	9	12	—	3
Lanzhou	7	9	7	4	6	—
Xi'an	8	10	10	4	6	3
Ningxia (Yinchuan)	7	12	7	4	6	3
Inner Mongolia (Xilinhot)	5	8	6	6	—	5
Beijing	15	21	8	5	—	3

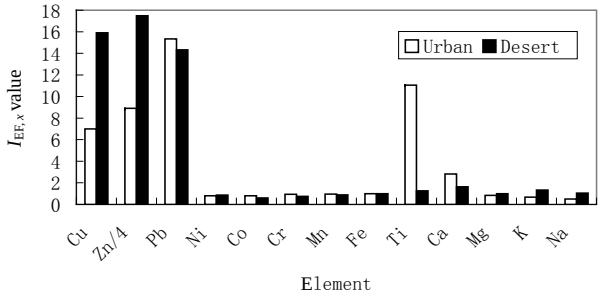

Fig. 3. $I_{\mathrm{EF},x}$ of various elements in dust samples obtained in Lanzhou (urban area) and Shaputo (desert area).

in suspension are in part the result of the concentration of clay matter, which increases the $I_{\mathrm{EF},x}$ value of some elements as the distance of transportation increases. Figure 3 contrasts $I_{\mathrm{EF},x}$ values in a desert area (Shaputo) from those in an urban area (Lanzhou), suggesting that the elevated $I_{\mathrm{EF},x}$ values for Cu, Zn, and Pb were related to air pollutants of industrial origin in the urban setting.

4.3 *Mineralogical characteristics of dust*

The mineralogical content of dust can be representative of local conditions or of aeolian contributions. For samples obtained in the desert region, the X-ray power diffractogram of the dust reveals a predominance of chlorite, illite, calcite, dolomite, gypsum, and zeolite (Table 5). The mineral content of dust varies according to where it was sampled, with coarser dust consisting primarily of carbonates, whereas mica and clay minerals predominated in fine dust (Table 5).

Sampled settled-out dust showed light-mineral content as high as 90%, relative to the total minerals present. In aeolian sediments, the heavy-mineral content was lower than in dust, accounting for only 5% of the total minerals. This seems counterintuitive for we would have thought that rivers and dust/sand storms would be able carry heavier/denser particles, whereas particles settling out from the atmosphere would be lighter/less dense. In the Tarim basin of western China, the unstable mineral content of dust was as high as 45%, containing mainly hornblende, biotite, and augite. Some 55% of dust mineral content could be termed stable or highly stable, represented by epidote, zoisite, muscovite, garnet, and trace minerals including tremolite and actinolite. The light minerals of dust from the Tarim basin were predominantly calcite, with the carbonate content reaching 5%–15%.

In eastern China, the unstable mineral content of the dust and surface sand was only 30%, lower than that in western China. The opaque metal mineral content of the eastern regions twice that in the western regions. In western China, hornblende content in dust was lower than in western China, but the epidote content was higher than in western China.

A semi-quantitative estimate of the relative amounts of the dominant minerals by XRD is shown in Table 5. The major minerals of dust sediments consisted of quartz, feldspar, chlorite, illite, calcite, dolomite, and zeolite. However, there were differences in their mineral composition. Besides quartz, dust samples from Kashi, Dunhuang, Ningxia, and Beijing contained large quantities of illite, while the Kashi and Xi'an dust contained sizable quantities of calcite. On the other hand, the Kashi, Dunhuang, and Kunlun mountain dust bore large quantities of dolomite, while the Inner Mongolia and Tarim dust bore large quantities of feldspar.

4.4 *Size distribution characteristics*

Size distribution by mass and by number were analyzed for the Ningxia samples. Mass concentration and number concentration aerosol spectra were generated in Ningxia (Yinchuan station) during both clear sky conditions, i.e., background (Figs. 4a, c), and a dust storm (Figs. 4b, d). The mass concentration spectrum for background conditions shows a triple peak pattern (Fig. 4a), with peak diameters of 0.67, 3.0, and 7.7 μm, respectively. The overall mass spectrum

coincides with a lognormal distribution through the three corresponding peak value diameters. The mass concentration spectrum under dust storm conditions (Fig. 4b) shows a single peak concurring with the report by Shao and Shi (2003), with a geometric mean diameter of mass concentration of 3.09 μm. A similar pattern of peaks and differences between clear sky and dust storm conditions was observed by You et al. (1991). The mass spectrum under dust storm conditions follows a lognormal distribution. The diameter at the peak value is 0.67 μm, and the distribution follows a typical T-distribution. Some 85% of sand dust particles exhibited a value of $d < 1$ μm, and the total mass concentration was 38.3 μg m^{-3}. The geometric mean diameter was thus 1.56 μm (Fig. 4d). Furthermore, only 23.6% of sand dust particles showed values of $d < 1$ μm, and the total mass concentration was 4428 μg m^{-3}.

The number concentration spectrum of the aerosol under clear sky conditions shows a typical single peak pattern and can be fitted with a T-distribution (Fig. 4c). And the number concentration of the aerosols is very low, only 12.6 particles cm^{-3} (Fig. 4c). Under these conditions, the peak value is comparatively stable, staying at 0.64–0.84 μm according to topography and geographic location. During dust storm episodes, the peak value for the number concentration spectrum increases with the intensity of the dust storm; in this investigation, the peak value of the aerosol diameter was 1.1 μm and it follows a lognormal distribution.

5. Conclusion

Wind erosion of silty and clayey material in the

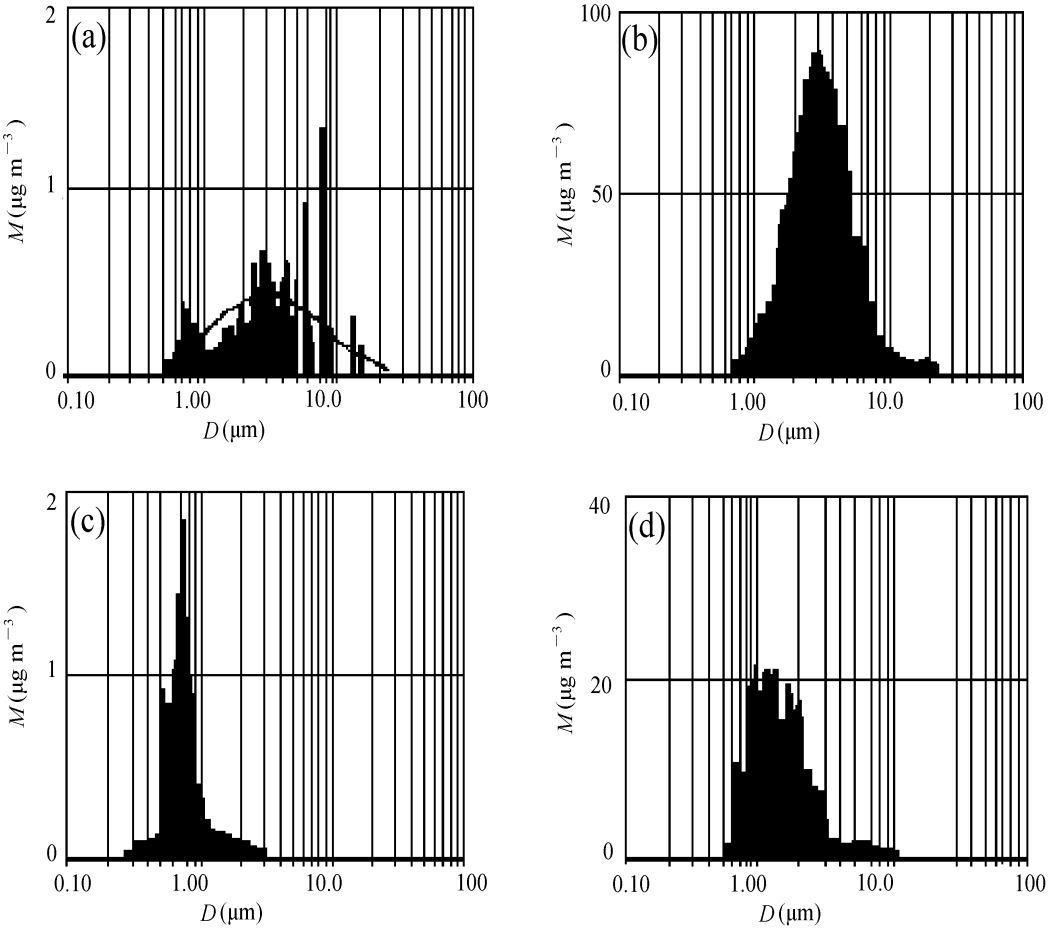

Fig. 4. Mass (a and b) and number (c and d) concentration spectra of aerosols sampled at Yinchuan, China. Spectra for clear weather are presented on the left (a and c) and for dust storm conditions on the right (b and d). The particle concentration is assumed to be 1.0 g m^{-3}, or 2.7 g m^{-3} should it be converted into actual mass of sand dust. D and M are particles diameter of sand dust (μm), particles number of sand dust (μg m^{-3}), respectively.

northwestern deserts and Inner Mongolia sandy lands and nearby dry lands is the source of the peri-desert dust deposits and loess soil in China. Studies of recent dust fall events in eastern China have given support to the hypothesis of the deposition of aeolian dust originating from western and central China. It is probably an important contributor to soil formation, slope wash, and stream sediments in eastern China and nearby seas. The $I_{\mathrm{EF},x}$ of elements in dust samples collected in some areas of China show that the main elements of airborne particulate matter correspond with aeolian fine sand and clay of on-site or nearby origin. Further evidence comes from the similarity in pattern of element distribution in clay from desert areas and in airborne particulate matter.

The major minerals of dust sediments consisted of chlorite, illite, calcite, feldspar, dolomite, and zeolite. However, there were differences in their mineral composition. The Kashi, Dunhuang, and Kunlun Mountains samples contained a relatively large quantity of dolomite, whereas those from Inner Mongolia and Tarim dust contained a relatively large quantity of feldspar.

The number concentration spectrum of dust in these areas was all of the one-peak type. Values for the three mass spectrum peaks, which occurred under clear sky conditions, were stable. Under dust storm conditions, these peaks merged, and the resulting single peak value increased with storm intensity. The number concentration spectrum, the surface area spectrum, and the mass spectrum all followed lognormal distributions. The quantitative role of eastern dust inputs, its history, and distribution in time and space should be the subject of further research.

Acknowledgments. The authors owe thanks to two anonymous reviewers for their invaluable comments. We are also grateful particularly thanks to Prof. Shao Longyi for his comments. This research was supported by the National 973 (TG2000048705), the Hundred Talent Scholar Foundation (Grant No.2003401), the Key Projects (KZCX1-09-03) and (KZCX1-10-06) of the Chinese Academy of Sciences, and the National Natural Science Foundation of China (Grant No. 40171007).

REFERENCES

An Zhisheng, and Liu Dongsheng, 1984: Long-term climatic change in the loess-plateau of China. *The climatic of China and global climate*, China Ocean Press, Beijing, 2–15. (in Chinese)

An Zhisheng, Liu Dongsheng, Lou Yunchang, S. C. Porter, and G. Kukla, 1990: The long-term paleomonsoon variation recorded by the loess-paleosols sequence in central China. *Quaternary International*, Volume 7–8, 91–95.

Chen, M. l., 1993: The study of dust storm weather in China. *Proc. Chinese Symposium on the Dust Storm Weather*, China Meteorological Administration, Lanzhou, 15–20. (in Chinese)

Davenport, W .H., 1949: Determination of aluminum in presence of iron-spectrophotometric method using ferron. *Analytical Chemistry*, **21**, 710–711.

Davis, B. J., and J. Guo, 2000: Airbone particulate study in five cities of China. *Atmospheric Environment*, **34**, 2703–2711.

Fan, X. B., K. K. Okada, N. R. K. Nimura, K. J. Kai, and K. M. Arao, 1996: Mineral particles collected in China and Japan during the same Asian dust-storm event. *Atmospheric Environment,* **30**, 347–251.

Feng Qi, Liu Wei, Liu Yansui, Zhang Yanwu, Su Yanghong, 2004: Impact of desertification and global warming on soil carbon in northern China. *Journal of Geophysical Research*, **109**(D2), D02104, doi:10.1029/2003JD003599.

Goudie, A. S., 1978: Dust storms and their geomorphologic implications. *Journal of Arid Environment*, **1**, 291–310.

Inoue, K., and T. Naruse, 1987: Physical, chemical, and mineralogical characteristics of modern aeolian dust in Japan and rate of dust deposition. *Soil Science Plant Nutrition.*, **33**(3), 327–345.

Li Xingsheng, Zhou Jianqiang, Li Zhe, Fang Xiumei, He Zhuanshi, and Farn Parungo, 1998: A numerical simulation of "5.5" super-dust storm in Northern China. *Adv. Atmos. Sci.*, **15**, 63–65.

Liu Dongsheng, 1964: *Loess Deposits in China.* Science Press, Beijing, 71pp. (in Chinese)

Liu Dongsheng, 1982: *The dusts fall in Beijing of the People's Republic of China on April 18, 1980.* American Geological Society (Special paper), 189pp.

Liu Dongsheng, 1985: *Loess and Environment in China.* Science Press, Beijing, 206pp. (in Chinese)

Mehlich, A., 1984: Mehlich No. 3 soil test extractant: A modification of Mehlich No. 2 extractant. *Communications in Soil Science and Plant Analysis*, **15**, 1409–1416.

Meigs, P., 1953: World distribution of arid and semi-arid climates. Review of research on arid zone hydrology. UNESCO, Paris. *Arid Zone Programs*, **1**, 203–210.

Middleton, N. J., A. S. Goudie, and G. L. Wells, 1986: The frequency and source areas of dust storms. *Aeolian Geomorphology*, Nickling et al., Eds., Boston, Massachusetts, 237–260.

Naruse, T., H. Sakai, and K. Inoue, 1986: Aeolians dust origin of fine quartz in selected soils, Japan, *Quaternary Research* (*Tokyo*), **24**, 295–300.

Péwé T. L. 1981: Desert dust: An overview. Desert dust: Origin, Characteristics, and Effect on Man. T. L. Péwé, Ed., *Geological Society of American Special Paper,* **186**, 1–10.

Prospero, J. M., R. T. Nees, and M. Uematsu, 1987: Deposition rate of particulate and dissolved aluminum derived from Saharan dust in precipitation at Miami, Florida. *J. Geophys. Res.*, **92**, 14723–14731.

Pye, K., 1987: *Aeolian Dust and Dust Deposits.* Academic Press, San Diego, Calif., 334pp.

Qian Zhengan, Qu Zhang, and Chen Mingli, 1997: Sandstorm classification critical, special spectrums and its statistic characteristics in Northwest China. *Research on Chinese Dust Storm*, Fang Zongyi, Ed., Sciences Press, Beijing 157pp. (in Chinese)

Shao Longyi, and Shi Zongbo, 2003: Microscopic characteristics and size distribution of summer PM_{10} in the air of a northwestern urban and a clean air site in Beijing. *Environmental Sciences*, **24**(5), 11–16. (in Chinese)

Shi Zongbo, Shao Longyi, T. P. Jone, A. G. Whittaker, Lu Senling, K. A. Berube, He Taoe, and R. J. Richards, 2003: Characterization of airborne individual particles collected in an urban area, a satellite city and a clean air area in Beijing, 2001. *Atmospheric Environment*, **37**, 4097–4108.

Smart, P., and K. Tovery, 1981: *Electron Microscopy of Soils and Sediments*. Oxford University Press, New York, 178pp.

Wang, J. Y., 1963: *Historical Records in Geology of China*. Science Press, Beijing, 269pp. (in Chinese)

Yaalon, D. H., and E. Ganor, 1973: The influence of dust on soils during the Quaternary. *Soil Sciences*, **116**, 146–155.

Yaalon, D. H., and J. Dan, 1974: Accumulation and distribution of loess-derived deposits in the semi-desert and desert fringe area of Israel. *Zeitschrift für Geomorphologie Supplementband* (Suppl.), **20**, 91–105.

Yamazaki, H., S. Gohda, K. Yokota, and T. Shirasaki, 2001: Quantitative assessment of chemical characteristics of the sediments in Lake Biwa Japan, by cluster analysis. Analytical Sciences, **17**, 1565–1567.

You, L. G., Ma, P. M., Chen, J. H., Li, K., 1991: A case study of the aerosol characteristics in the lower troposphere during a dust storm event. *Chinese Quarterly Journal of Applied Meteorology*, **2**(1), 13–22. (in Chinese)

Zhang Deer, 1980: Winter temperature change during the last 500 years in southern China. *Chinese Science Bull*, **6**.

Zhang, X. Y., Z. S. An, T. Chen, G. Y. Zhang, R. Arimoto, and Y. B. Ra, 1994: Late Quaternary records of the atmospheric input of aeolian dust to the center of the Chinese Loess Plateau. *Quternary Research*, **41**, 35–43.

Zhang, X. Y., R. Arimoto, and Z. S. An, 1999: Glacial and interglacial patterns for Asian dust transport. *Quaternary Sciences Review*, **12**, 811–819.

Zhen, S. Z., 1973: Humidity condition in southeastern China for the last 2000 years. *Proc. Climatic Change and Ultra-long Range Weather Forecasting*. Science Press, Beijing, 29–32. (in Chinese)

Zhu Zhenda, Cheng Guangting, 1994: *Sandy Land Desertification and in China*. Science Press, Beijing, 250pp. (in Chinese)